5-4-2004

Experimental and Theoretical Studies on the Pharmacodynamics of Cisplatin in Jurkat Cells

Kirk A. Tacka
Syracuse University

Dava Szalda
Syracuse University

Abdul-Kader Souid
State University of New York

Jerry Goodisman
Syracuse University

James C. Dabrowiak
Syracuse University

Recommended Citation

Tacka, K. A., Szalda, D., Souid, A. -., Goodisman, J., & Dabrowiak, J. C. (2004). Experimental and theoretical studies on the pharmacodynamics of cisplatin in jurkat cells. Chemical Research in Toxicology, 17(11), 1434-1444.

Experimental and Theoretical Studies on the Pharmacodynamics of Cisplatin in Jurkat Cells

Kirk A. Tacka,[†] Dava Szalda,[‡] Abdul-Kader Souid,[§] Jerry Goodisman,[†] and James C. Dabrowiak*,[†]

Departments of Chemistry and Bioengineering and Neuroscience, Syracuse University, 111 College Place, CST Rm1-014, Syracuse, New York 13244-4100, and Department of Pediatrics, Upstate Medical University, State University of New York, 750 East Adams Street, Syracuse, New York 13210

Received May 4, 2004

For Jurkat cells in culture exposed to cisplatin (**1**), we measured the number of platinum adducts on DNA and showed that it is proportional to the AUC, the area under the concentration vs time curve, for cisplatin. The number of platinum−DNA adducts is measured immediately following exposure to drug. The AUC is calculated either as the product of the initial cisplatin concentration and the exposure time or as the integral under the concentration vs time curve for the unreacted dichloro species, which decreases exponentially. We also show that the number of adducts correlates with decreases in respiration, with the amount of DNA fragmentation, and with cell viability, all measured 24 h after exposure to the drug. To study the reactions of cisplatin at concentrations approaching clinical relevance (65 μM), we use two-dimensional [^{1}H^{15}N]HSQC NMR and the ^{15}N-labeled form of the drug, *cis*-Pt($^{15}NH_3$)$_2$Cl$_2$, **1**. In the absence of cells, **1** reacts with components of the growth medium and also transforms slowly (k_h = 0.205 h^{-1} at 37 °C) into the chloro-aquo species, *cis*-[Pt($^{15}NH_3$)$_2$Cl(H_2O)]$^+$ (**2**), which at the pH of the medium (pH 7.15), is mainly in the deprotonated chloro-hydroxy form, *cis*-Pt($^{15}NH_3$)$_2$-Cl(OH) (**4**). The concentration of **2** (**4**), as measured by HSQC NMR, decreases due to reaction with components of the medium. In the presence of 5 million or more cells, the concentration of **1** decreases with time, but the NMR signal for **2** (**4**) is not seen because it is rapidly removed from solution by the cells, keeping its concentration very low. These experiments confirm that the species preferentially removed from the medium by cells is **2** (**4**) and not **1**. Our findings are discussed in the context of a kinetic model for platination of nuclear DNA by cisplatin, which includes aquation of cisplatin outside the cell, passage of **2** (**4**) through the cell membrane, reaction of reactive platinum species (RPS) in the cytosol with thiols, formation of adducts between RPS and accessible sites on genomic DNA, and removal of platinum from DNA by repair. Some of the rate constants involved are measured, but others can only be estimated. Calculations with this model show that little of the platinum reacts with intracellular thiols before reaching the nuclear DNA, indicating that binding to thiols is not important in cisplatin resistance. The model also predicts the circumstances under which the amount of platination of nuclear DNA is proportional to AUC.

Introduction

Cisplatin, *cis*-dichlorodiammineplatinum (II),[1] is in wide clinical use for the treatment of a variety of cancers (*1*). A major problem with cisplatin therapy is the resistance associated with extended use of the drug (*2*). Because cisplatin-induced apoptosis is related to the amount of platinum (Pt) bound to genomic DNA, cellular mechanisms that reduce the number of Pt−DNA adducts are the main factors affecting cisplatin resistance. These include DNA repair (*2*, *3*), efflux of Pt from cells (*4*−*6*), and reaction of the drug with glutathione (GSH) and metallothionein (MT) (*2*, *7*−*9*). More recently, it has been shown that other biochemical processes, not directly related to platination of DNA, may also contribute to resistance. For example, thiolate adducts of cisplatin that form in the cytoplasm may affect the thiol/disulfide equilibrium thus blocking the cell from entering into apoptosis (*10*−*12*).

For cell cycle nonspecific drugs such as cisplatin, Ozawa et al. (*13*) showed that cytotoxicity is proportional to the product of the exposure time and extracellular drug concentration, referred to as the area under the curve or AUC. It is often the case that AUC is the important parameter in determining the antitumor activity of cisplatin and other drugs (*14*−*17*) although exceptions

* To whom correspondence should be addressed. Tel: 315-443-4601. Fax: 315-443-4070. E-mail: jcdabrow@syr.edu.
[†] Department of Chemistry, Syracuse University.
[‡] Department of Bioengineering and Neuroscience, Syracuse University.
[§] State University of New York.

[1] Abbreviations: cisplatin, *cis*-diamminedichloroplatinum(II), *cis*-Pt(NH_3)$_2$Cl$_2$; [O_2], oxygen concentration; [cisplatin], cisplatin concentration; AAS, atomic absorption spectroscopy; RT, room temperature; Pd phosphor, palladium(II) complex of *meso*-tetra(4-sulfonatophenyl)-tetrabenzoporphyrin; BSA, bovine serum albumin; dH_2O, distilled deionized water; D_2O, deuterium oxide; FBS, fetal bovine serum; PBS, phosphate-buffered saline; Pt, platinum; TBE, Tris−borate−EDTA; bp, base pair; kb, kilo base pair; nt, nucleotide; AUC, area under curve; GSH, glutathione; MT, metallothionein; HSQC, heteronuclear single quantum cohearence; RPS, reactive platinum species.

10.1021/tx0498760 CCC: $27.50
Published on Web 10/13/2004

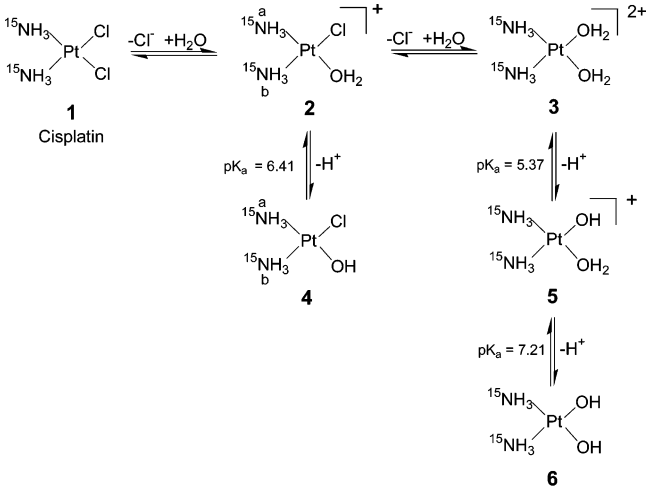

Figure 1. Aquation of cisplatin. The values for the pK_a values are from ref *31*.

are also well-known (*18*, *19*). In addition to establishing the validity of AUC for cisplatin in different cell types, modeling the cytotoxicity of the drug using experimental rate data for binding/transfer events in the cell has also been attempted. Miyagi et al. (*20*) constructed a model to explain the cytocidal and DNA binding effects of nedaplatin, a cisplatin analogue. Their model included drug transport across the cell membrane and drug reaction with DNA and assumed cell death occurred when the percentage of DNA−Pt adducts exceeded a threshold. Assuming rate constants for the processes, the coupled differential equations were solved to obtain the percent of cells killed as a function of time and drug concentration in the extracellular fluid. In modeling cisplatin cytotoxicity, El-Kareh and Secomb (*18*) considered the uptake, efflux, DNA binding, and repair rates of the drug to produce a model that provided good fits to experimental data sets, including exposure times of ∼100 h. Recently, we proposed a model for cisplatin binding to genomic DNA (*21*). Our model included transfer of cisplatin across the cell and nuclear membranes, platination of DNA, and reaction of cisplatin with cellular thiols and cellular drugs. The amount of Pt bound to DNA was calculated by solving coupled differential equations, assuming values for rate constants that gave agreement between calculated and measured results, since measured values for some of them were not available.

In an earlier study (*22*), we showed that alteration in mitochondrial function is a secondary effect of cisplatin cytotoxicity in Jurkat cells in culture. In this report, we simulate continuous injection of cisplatin by exposing Jurkat cells to different concentrations of the drug for different periods of time. We show that the AUC correlates with the amount of Pt bound to DNA immediately after drug exposure and with changes in cellular respiration, viability, and DNA fragmentation observed 24 h after exposure. Using two-dimensional (2D) [^{1}H^{15}N] heteronuclear single quantum cohearence (HSQC) NMR and the ^{15}N-labeled form of the drug, *cis*-Pt($^{15}NH_3$)$_2$Cl$_2$ (**1**) (Figure 1), we identify the cisplatin species preferentially removed from the culture medium by the cells. Although not so far employed for cell studies involving cisplatin, HSQC NMR has been used to characterize solution chemistry and reaction products of cisplatin and some of its analogues (*23*−*31*). We find that in the cell culture medium at pH 7.15, cisplatin aquates to produce the chloro-aquo complex, *cis*-[Pt($^{15}NH_3$)$_2$(H$_2$O)Cl]$^+$ (**2**), which is in equilibrium with the chloro-hydroxy compound, *cis*-Pt($^{15}NH_3$)$_2$(OH)Cl (**4**) (Figure 1). The HSQC NMR studies show that compared to **1**, the mono-aquated product, **2** (**4**), is more readily removed from the medium by the cells.

This and other information are used to improve our kinetic model of Pt binding to genomic DNA. The aquation of **1** to **2** is included (the rate constant is known) as well as the uptake of **2** and **4** by cells (with measured rate constants). In addition to helping to explain Pt binding to DNA and the AUC data, the model should provide a framework for understanding Pt cytotoxicity to cancer and normal cells. Suitably parametrized, it could then be used to suggest dosing protocols for Pt anticancer drugs, which maximize cancer cell kill while minimizing damage to normal cells.

Materials and Methods

Chemicals. All materials were reagent grade and used as supplied. Cisplatin (3.3 mM in 154 mM aqueous NaCl) was obtained from American Pharmaceutical Partners (Los Angeles, CA); the Pd(II) complex of *meso*-tetra(4-sulfonatophenyl)tetrabenzoporphyrin (Pd phosphor), sodium salt, was purchased from Porphyrin Products, Inc. (Logan, UT); proteinase k, ribonuclease A (DNase-free from bovine pancreas; contained ∼80 units/mg), rotenone, adenosine 5′-diphosphate (ADP), bromophenol blue, xylene cyanol FF, and fatty acid free bovine serum albumin (BSA) were purchased from Sigma-Aldrich (St. Louis, MO); nonyl phenyl-poly(ethylene glycol) (Nonidet NP-40) was purchased from Fluka (Ronkonkoma, NY); agarose (molecular biology grade) was purchased from Promega (Madison, WI); Dulbecco's phosphate-buffered saline (PBS; w/o calcium or magnesium), fetal bovine serum (FBS), and RPMI-1640 medium with L-glutamine (pH 7.15) were purchased from Mediatech (Herndon, VA); DNA HyperLadder I [200−10 000 base pair (bp)] was purchased from Bioline USA Inc. (Randolph, MA). *cis*-Pt($^{15}NH_3$)$_2$Cl$_2$ was synthesized from K_2PtCl_4 (Sigma-Aldrich) and $^{15}NH_4CO_2CH_3$ (Cambridge Isotope Laboratories, Inc., Andover, MA) using an earlier reported procedure (*32*). The ^{15}N-labeled drug was recryctallized from boiling 0.1 M HCl.

Solutions. The Pd phosphor for the respiration studies was dissolved in distilled deionized water (dH$_2$O) (2.5 mg/mL or ∼2.0 mM) and stored in the refrigerator for less than 2 weeks. Rotenone (1.0 mM) was freshly dissolved in absolute ethanol. Phosphate-citrate buffer consisted of 200 mM Na_2HPO_4, with the pH adjusted to 7.8 with 0.1 M citric acid. Proteinase k (20 mg/mL) and ribonuclease A (10 mg/mL) solutions were made in dH$_2$O and stored at −20°C. Nonidet NP-40 0.25% (v/v) solution was made in dH$_2$O and stored at room temperature (RT). Gel loading buffer contained (v/v) 0.25% bromophenol blue, 0.25% xylene cyanol FF, and 30% glycerol in dH$_2$O. Tris−borate−EDTA (TBE) buffer contained 40 mM Tris, boric acid, and 2 mM EDTA (pH 8.3).

The Pd phosphor solution for the respiration experiments contained 2 μM Pd phosphor, 2% (w/v) BSA, and 5 mM ADP in RPMI (containing ∼6 mM Na_2HPO_4 and 10 mM glucose); the final pH was ∼7.5. The solution was freshly made in a 30 mL quartz tube and continuously stirred for at least 90 min prior to use.

Cells. The human T-cell lymphoma cell line, Jurkat, was a gift from Dr. Edward Barker. The cells were maintained in suspension culture under a fully humidified atmosphere containing 5% CO_2 at 37 °C. The medium was RPMI-1640 supplemented with 10% (v/v) FBS, 100 μg/mL streptomycin, 100 IU/mL penicillin, and 2.0 mM L-glutamine. The number of cells and their viability were determined immediately prior to experimental measurements by light microscopy, using a hemacytometer under standard trypan blue staining conditions (*33*).

Table 1. Effect of AUC on Cisplatin Cytotoxicity in Jurkat Cells[a]

initial [cisplatin] (μM)	exposure time (h)	AUC (μM × h)	Pt−DNA adducts per 10^6 nt	viability (%)	k (μM O_2 min^{-1} per 10^6 cells)	DNA fragment intensity
0	3.0	0	4.7 ± 2.7	96 ± 2.0	0.37 ± 0.12	9.6 ± 3.1
5	3.0	11.2	9.0 ± 3.5	91 ± 1.0	0.38 ± 0.18	13.1 ± 6.2
10	1.5	12.9	5.9 ± 1.6	92 ± 0.6	0.33 ± 0.09	14.1 ± 6.8
15	1.0	13.6	6.7 ± 1.5	93 ± 3.0	0.33 ± 0.07	14.1 ± 7.4
15	3.0	33.6	24.9 ± 8.0	83 ± 1.0	0.18 ± 0.00	30.6 ± 4.8
30	1.5	38.7	26.3 ± 5.0	86 ± 1.7	0.20 ± 0.01	28.6 ± 1.2
45	1.0	40.7	27.6 ± 15.0	86 ± 3.5	0.22 ± 0.03	26.9 ± 9.0
25	3.0	56.0	46.7 ± 11.8	70 ± 4.4	0.15 ± 0.02	36.5 ± 0.8
50	1.5	64.6	37.5 ± 10.6	76 ± 4.4	0.13 ± 0.01	29.0 ± 9.5
75	1.0	67.8	36.5 ± 12.0	76 ± 2.6	0.17 ± 0.01	37.4 ± 5.5

[a] Cells (~10^7 per condition) were incubated at 37 °C with the indicated [cisplatin] for the indicated period of time. At the end of the incubation periods, the cells were collected by centrifugation, washed, and analyzed immediately for Pt−DNA adducts or maintained in culture (drug-free medium) and analyzed 24 h later, for respiration, viability, and DNA fragmentation as described in the Materials and Methods. The numbers are the means ± SD of 2−3 experiments.

Incubation of Cells with Cisplatin. Incubations were carried out in RPMI medium plus 10% FBS at 37 °C. Cells in logarithmic growth (~10^7/condition) were exposed to cisplatin using times and drug concentrations indicated in Table 1. At the end of the incubation periods, the cells were collected by centrifugation, washed, and analyzed immediately for Pt−DNA adducts or maintained in culture (drug-free medium) and analyzed 24 h later, for respiration, viability, and DNA fragmentation.

Pt−DNA Adducts. Cellular (genomic) DNA was extracted from Jurkat cells immediately following the incubations with cisplatin. Pt−DNA adducts per 10^6 nucleotides (nts) (Table 1) were determined by atomic absorption spectroscopy (AAS) as previously described (*21*).

Cellular Oxygen Consumption. Respiration was measured at RT in sealed vials containing cells suspended in 0.7 mL of the Pd phosphor solution 24 h after exposure to cisplatin. The substrate for the cells was glucose. The concentration of oxygen [O_2] in the solution was measured as a function of time using the phosphorescence probe, Pd phosphor (*34*, *35*). This method was based on oxygen quenching of phosphorescence of the Pd phosphor.

The rate of cellular mitochondrial oxygen consumption (μM O_2 min^{-1}) was calculated as the negative slope of the linear portion ([O_2] ≥ 150 μM) of the [O_2] vs time curves. The value of k, a zero-order rate constant, was set equal to the negative slope of each curve divided by the total number of cells (in millions) in each sample. Each experiment included a measurement in the presence of rotenone (which inhibits complex I of the respiratory chain). The rate of oxygen consumption for the Pd phosphor solution without cells was (mean ± SD) 0.28 ± 0.05 μM O_2 min^{-1} and, for ~10^7 cells incubated with rotenone (50 μM at 37 °C for 1 h), 0.36 ± 0.16 μM O_2 min^{-1}.

Extraction of DNA Fragments. DNA fragments were extracted as described (*36*) with some modifications. Cells were washed with PBS and suspended in 1.0 mL of ice-cold PBS. Cells (~3 × 10^6/condition) were fixed in 8.0 mL of ice-cold 70% ethanol. The suspension was incubated at −20 °C for 24 h and then centrifuged (1000*g* for 5 min at 4 °C). The supernatant was discarded, and the ethanol was allowed to completely evaporate at RT. The pellet was suspended in 50 μL of phosphate-citrate buffer and incubated at 20 °C for 90 min. The suspension was centrifuged (as above), and the supernatant was transferred to a fresh tube. The supernatant was recentrifuged as above, and the supernatant was lyophilized in a Speed Vac. The lyophilized pellet was suspended in 6 μL of Nonidet NP-40 (0.25% solution), 6 μL of SDS (10%), 6 μL of ribonuclease A (10 mg/mL solution), and 2 μL of ribonuclease T_1. After overnight incubation at 37 °C, 6 μL of proteinase k (20 mg/mL solution) was added and the mixture was incubated overnight. Twenty-four microliters of the gel-loading buffer was added (final volume ~50 μL).

Agarose Gel Electrophoresis. Approximately 22 μL of the above extract was loaded on 4 mm thick, 1.0% agarose gels, and electrophoresed at 25 V and 11 mA for ~15 h in TBE buffer. Each extract was loaded on two separated gels. The gels were stained in 300 mL of 0.5 μg/mL ethidium bromide for 30 min in the dark at RT. After destaining for 15 min in dH_2O, the gels were stored at 4 °C in 300 mL of TBE. The images were captured using a Gel Doc digital camera system with Quantity One software (Bio-Rad, Richmond, CA).

Quantitation of Stained Gels. The digital image of the stained gel was captured after adjusting the exposure time and iris diaphragm of the camera so that the maximum pixel intensity was below saturation (*22*). The digital image was analyzed using Sigma Scan software (version 2.0, SPSS Inc.). Individual lanes were scanned from the loading well to the low molecular weight end of the streaks. Net intensity vs position plots were exported to Peak-Fit software (version 4.1, SPSS Inc.), and the total intensity in the range of 0.1−10.0 kilo base pair (kb) (in arbitrary units) for each lane was determined.

HSQC NMR. The 2D [$^1H^{15}N$]HSQC NMR spectra were recorded at 37 °C using Bruker ADVANCE 500 and 600 spectrometers equipped with triple axes probes. The frequencies used were as follows: ^1H, 500.13 and 600.13 MHz; ^{15}N, 50.646 and 60.81 MHz. The spectra, optimized for $^1J(^{15}N-^1H) = 72$ Hz, were recorded using a pulse sequence available in the Bruker software package. The NMR experiment was 2D, $^1H-^{15}N$, with inverse detection, phase sensitive with ECHO/Antiecho-TPP1 gradient selection, with decoupling during acquisition. Samples were not spun during the experiment. Twenty NMR experiments (each 62 min in length, ns = 48) were conducted for each kinetic run with **1**. For each NMR experiment, there were 1K data points in the proton dimension and 64 t_1 values. The sweep widths in the proton and nitrogen dimensions were 4006.41 (8.01 ppm) and 4054.06 (80 ppm), respectively. Processing included squared cosine apodization in both dimensions, and zerofilling along the remote dimension to create a symmetric matrix (1K × 1K). For some experiments, 15 to −115 ppm on the ^{15}N axis was searched. Peak volumes [the ^{195}Pt satellites of *cis*-Pt($^{15}NH_3$)Cl_2 were not included] were calculated using Bruker software, and the volumes analyzed in the manner described in the text.

The ^{15}N chemical shifts were referenced externally to 1 M $(^{15}NH_4)_2SO_4$, in 95/5 H_2O/deuterium oxide (D_2O), which was acidified to pH ~1 by addition of H_2SO_4. The ^1H chemical shift of **1** relative to $Me_3SiCD_2CD_2CO_2Na$, TSP, in a pH 7.15, 23 mM sodium bicarbonate buffer, was 4.09 ppm.

Each NMR sample was prepared so that it contained 5% added D_2O. This permitted locking onto deuterium with minimal loss of the signal intensity from hydrogen/deuterium exchange of the Pt complexes. The NMR studies were carried out in RPMI-1640 (pH 7.15) supplemented with 10% (v/v) FBS, 100 μg/mL streptomycin, 100 IU/mL penicillin, and 2.0 mM L-glutamine. The chloride concentration in the medium was ~105 mM, and the final volume in the NMR tube was 920 μL. Concentrations of stock solutions of labeled cisplatin were determined by AAS.

The kinetics of reaction of cisplatin in the absence of cells was measured using a solution containing 65 μM *cis*-Pt($^{15}NH_3$)$_2$-Cl_2 (**1**) (Figure 1). The assignment of peaks that appear when **1** reacts in culture medium in the absence of cells was done by reference to the literature (*31*) and by collecting NMR data on solutions of cisplatin that were "aged" by allowing 4.2 mM **1** to stand for 24 h in 10 mM NaCl. This produces a mixture of **1** and its aquated forms **2** and **3** (*31*). A portion of the aged solution was added to the culture medium to give a concentration of 65 μM Pt, and NMR data for 1 h were obtained. The spectrum exhibited the same peaks as those observed when **1** hydrolyzes in culture medium, but the relative intensities of the peaks for **1** and **2** (**4**) were different, with more of the mono-aquo present in the aged samples. Peak assignments for the mono-aquated complex were further confirmed by determining the 2D HSQC NMR spectrum of an aged solution (described above) of cisplatin in 23 mM $NaHCO_3$ buffer (pH 7.15). Acidification of this solution with 1 N HNO_3 to values of pH in the range of 7.15 to ~5 produced NMR spectra consistent with the earlier published assignments for **2** and **4** (*31*). This also confirmed that at pH 7.15, the peaks for **1** and **4b** overlap.

The kinetics of reaction of cisplatin in the culture medium with ~1.5 × 10^7 cells was measured using a solution containing 65 μM **1**. The stock solution of drug in 154 mM aqueous NaCl was added to the cells in the medium, the suspension was mixed by pipet action, and the resulting mixture was added to the NMR tube.

On separate samples under NMR conditions in sealed tubes, cell viability was checked every hour for the first 8 h of the kinetic run and again at the end of the run, ~21 h. The viabilities of drug-treated and untreated cells were virtually the same, 91.8 ± 5.0 vs 94.7 ± 2.3%, respectively, during the first 8 h. At the end of the ~21 h exposure period, the viabilities were low but there was a measurable difference between untreated (27.5 ± 7.8%) and treated cells (10.0 ± 7.1%). Moreover, at the end of the ~21 h exposure period, untreated cells respired twice as fast and had ~50% fewer DNA fragments than cells treated with cisplatin under NMR-like conditions (data not shown).

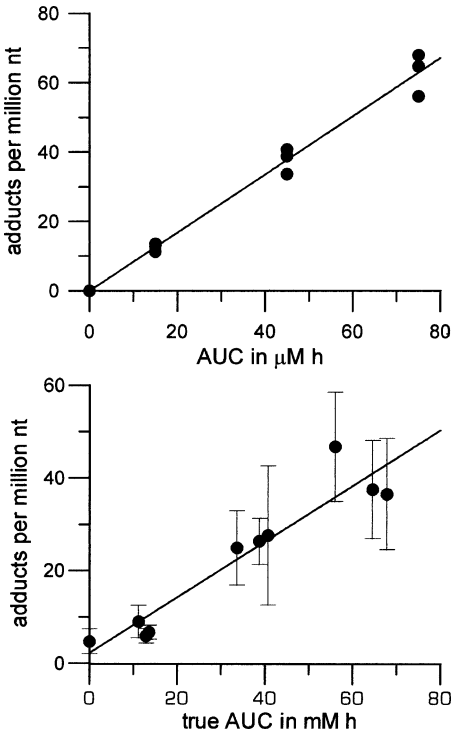

Figure 2. Dependence of DNA−Pt adduct formation on AUC. Two experiments were done with 15 million cells per condition, incubated at 37 °C for the times and cisplatin concentrations indicated in Table 1. The upper panel shows the number of Pt−DNA adducts in cells incubated with cisplatin solution vs AUC, calculated as the product of [cisplatin] C_C (μM) and exposure time T (h). The least-squares linear fit (dashed line) is = 0.52 + 1.40(AUC) with $R^2 = 0.95$. The lower panel shows the number of Pt−DNA adducts (with experimental error bars) vs true AUC, calculated as product of C_C and $(1 - e^{-kT})/k$, where k = 0.205 h^{-1}. The least-squares linear fit (dashed line) is 0.60 + 2.22-(AUC) with $R^2 = 0.91$.

Results

Effect of AUC on Pt−DNA Adduct Formation by Cisplatin. Pt−DNA adducts were measured at the end of the incubation periods indicated in Table 1. The amount of Pt−DNA adducts is plotted vs AUC, calculated as the product of the cisplatin concentration ([cisplatin]) (μM) and the exposure time (h), in Figure 2 (upper panel). DNA platination increased linearly with AUC (dashed line, $R^2 > 0.94$). Jurkat cells treated with an AUC = 15 μM h (5 μM for 3 h, 10 μM for 1.5 h, or 15 μM for 1 h) produced ~5.9−9.0 Pt adducts per 10^6 nts. For AUC = 45 μM h (15 μM for 3 h, 30 μM for 1.5 h, or 45 μM for 1 h), the amount of Pt−DNA adducts was 3−4 times higher, and for AUC = 75 μM h, DNA platination increased by a factor of 4−5.

The calculation of AUC as concentration × time, T, is appropriate when the [cisplatin] is maintained constant, as in administering the drug by infusion into plasma. However, the NMR results (see below) show that in our experiments, the concentration of **1** decreased exponentially, [cisplatin] = (65 μM) e^{-kt}, because of formation of the mono-aquated product **2** (**4**) and uptake of the latter by the cells, with a hydrolysis rate constant k_h of 0.205 h^{-1}. Thus, the AUC can also be calculated as $\int C\, dt = (C_C/k)(1 - e^{-kT})$ where C_C is the initial concentration of **1**. A plot of the amount of Pt−DNA adducts vs AUC calculated in this way ("true AUC") is shown in the lower panel of Figure 2, with the best linear fit. Although R^2 is slightly decreased (to 0.91), the fit is well within experimental error.

During the incubation periods with cisplatin, Pt−DNA adducts are continuously formed and removed (*1*, *2*). Inhibition of the nucleotide excision repair mechanism has been shown to increase adduct levels ~2-fold (*37*). Thus, the Pt−DNA adducts that we measured were a net value representing the difference between the number of adducts formed and the number of adducts removed by repair.

Effects of AUC on Cisplatin-Induced Impairments of Cellular Respiration, DNA Fragmentation, and Loss of Cell Viability. The dependence of cellular mitochondrial oxygen consumption (measured 24 h after drug exposure) on AUC is shown in Table 1. A representative [O_2] vs time curve for each AUC value is shown in Figure 3. The rate of respiration decreases linearly with AUC (0−67.8 μM h, $R > 0.95$).

The effects of the AUC on cisplatin-induced DNA fragmentation measured 24 h after exposure to the drug are summarized in Table 1 and shown in Figure 4. The amount of fragmented DNA increases almost linearly ($R > 0.94$) as a function of AUC. The percentage of viable cells (mean ± SD) 24 h after exposure to drug is also given in Table 1. The percentage of viable cells decreases linearly with $R > 0.96$ (plots not shown).

HSQC NMR. These experiments showed that the amount of Pt bound to DNA, as well as other cytotoxicity parameters described above, were proportional to AUC.

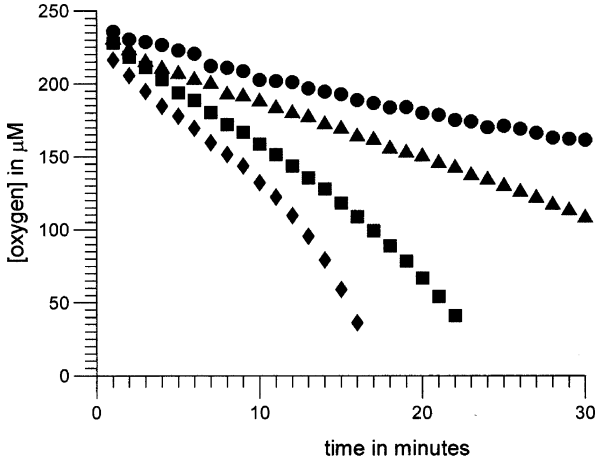

Figure 3. Dependence of AUC on cisplatin-induced mitochondrial dysfunction as measured by decreased cellular oxygen consumption. An oxygen consumption curve for each AUC value (0, diamonds; 13.6 μM h, squares; 38.7 μM h, triangles; and 56.0 μM h, circles) from a representative experiment is shown. Cells ($\sim 10^7$ per condition) were incubated at 37 °C for the times and cisplatin concentrations indicated in Table 1 and then maintained in drug-free medium for 24 h at 37 °C. At the end of the incubation period, a small volume of each suspension was removed to determine cell count and viability. The remaining cells were washed with PBS, suspended in the Pd phosphor solution, and placed in the instrument. The values of k were calculated as described in the Materials and Methods. The average (mean ± SD) values of k for each AUC value from three independent experiments are shown in Table 1.

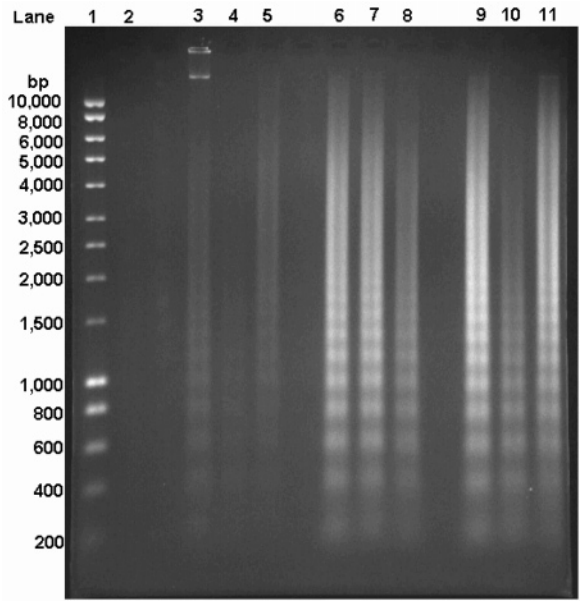

Figure 4. AUC dependence of cisplatin cytotoxicity as measured by DNA fragmentation. A representative gel is shown. The experimental conditions were as described in the legend to Table 1. Three experiments were done with results (mean ± SD) shown in Table 1. Lane 2 (from left): cells incubated with no addition for 3 h (AUC = 0). Lanes 3−5 are cells incubated with AUC = 11.2−13.6 μM h (lane 3, 5 μM, 3 h; lane 4, 10 μM, 1.5 h; and lane 5, 15 μM, 1 h). Lanes 6−8 correspond to AUC = 33.6−40.7 μM h (lane 6, 15 μM, 3 h; lane 7, 30 μM, 1.5 h; and lane 8, 45 μM, 1 h). Lanes 9−11 correspond to AUC = 56.0−67.8 μM h (lane 9, 25 μM, 3 h; lane 10, 50 μM, 1.5 h; and lane 11, 75 μM, 1 h). Lane 1 is a DNA HyperLadder I (200−10 000 bp).

The cisplatin species that formed in the culture medium were next identified using HSQC NMR. The addition of 65 μM *cis*-Pt($^{15}NH_3$)$_2$Cl$_2$ (**1**) to the cell culture medium without cells at 37 °C resulted in the slow disappearance

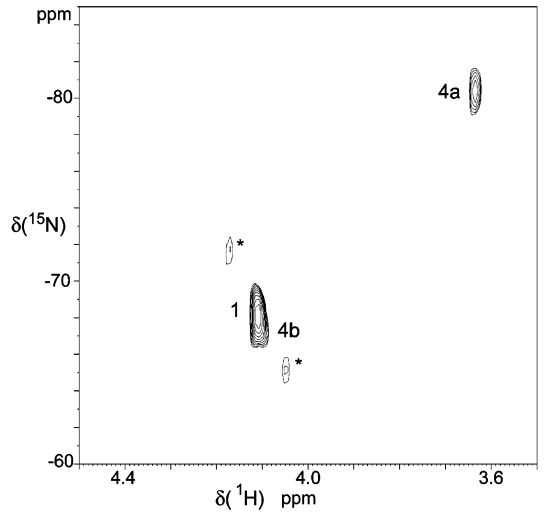

Figure 5. Two-dimensional [^{1}H,^{15}N]HSQC NMR (500 MHz) spectrum of 65 μM *cis*-Pt($^{15}NH_3$)$_2$Cl$_2$ in RPMI cell culture medium, pH 7.15, at 37° C. Compound **1** is *cis*-Pt($^{15}NH_3$)$_2$Cl$_2$, and compound **4** is *cis*-Pt($^{15}NH_3$)$_2$(OH)Cl. (a) $^{15}NH_3$ trans to OH; (b) $^{15}NH_3$ trans to Cl (see Figure 1 for structures). Asterisks show the ^{195}Pt satellites of **1**. The spectrum was obtained 3 h following the addition of **1** to the culture medium.

of the peak for **1** at ^{1}H/^{15}N, δ = 4.09/−68.0, and the appearance of a new peak at ^{1}H/^{15}N, δ = 3.61/−80.5 (Figure 5). On the basis of earlier published assignments (*31*) and NMR data collected on "aged" solutions of **1** in this work, the latter peak was assigned to $^{15}NH_3$ trans to the O of *cis*-Pt($^{15}NH_3$)$_2$(OH)Cl (**4**) (Figure 1). The peak for $^{15}NH_3$ trans to the Cl of **4** was at almost the same position as the peak for the two labeled ammonia molecules of **1** (*29*, *31*). This gives rise to the asymmetric peak at ^{1}H/^{15}N, δ = 4.09/−68.0 (Figure 5). Because the pK_a for the deprotonation of **2** to form **4** is 6.41 (*31*), at pH 7.15, the distribution of species is ∼15% **2** and ∼85% **4**.

In the culture medium without cells, the intensity of the cisplatin peak decreased exponentially with time (see Figure 6). The intensity of the peak assigned to the deprotonated aquated product **4** also decreased exponentially but more slowly. No peaks other than those for **1** and **4** were observed in the spectra. When 5 million or more cells are present, the intensity of the peak for **1** decreased with time (Figure 7), but the peak for **4** was not observed. A new peak (^{1}H/^{15}N, δ = 3.98/−62.0) of low intensity appeared after several hours.

To further confirm that the peak assignments shown in Figure 5 were correct, we measured the kinetics of decrease of **1** in the culture medium. The intensity (volume) of the peak at ^{1}H/^{15}N, δ = 3.61/−80.5, was subtracted from the intensity of the peak at δ = 4.09/−68.0, and the result was divided by 2 (two equal resonances present for **1**). Fitting the first nine points (t < 9 h) to an exponential gave 106.47 $e^{-0.205t}$, so that the value of the rate constant is k_h = 0.205 h^{-1} = 5.7 × 10^{-5} s^{-1} at 37 °C, somewhat higher than the reported rate constant for the hydrolysis of cisplatin at 25 °C, 5.18 × 10^{-5} s^{-1} (*29*).

Finally, we calculated the initial rate of decrease of [**1**] by subtracting the intensity of the peak at ^{1}H/^{15}N, δ = 3.61/−80.5, from that of the cisplatin peak at each time (t) and fitting the first six points to a line. Assuming the initial concentration of **1** was 65 μM, the three experiments shown in Figure 6 gave 5.6 ± 1.1, 7.9 ± 1.8, and

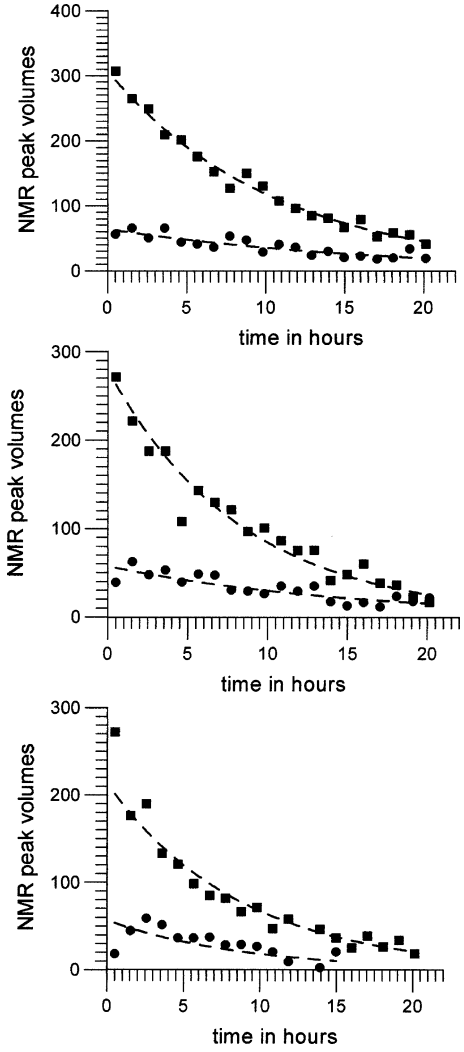

Figure 6. Integrated intensities (volumes) of NMR peaks as functions of time in the absence of cells in culture medium. The results of three experiments (65 μM, **1**) are shown. Squares = intensities for peak at $^{1}H/^{15}N$, $\delta = 4.09/-68.0$, due to **1**, and the ammonia molecule trans to the Cl of **4**; circles = intensities for peak at $^{1}H/^{15}N$, $\delta = 3.61/-80.5$, due to the ammonia molecule trans to the OH of **4**; and dashed lines = fit of intensities to exponentials.

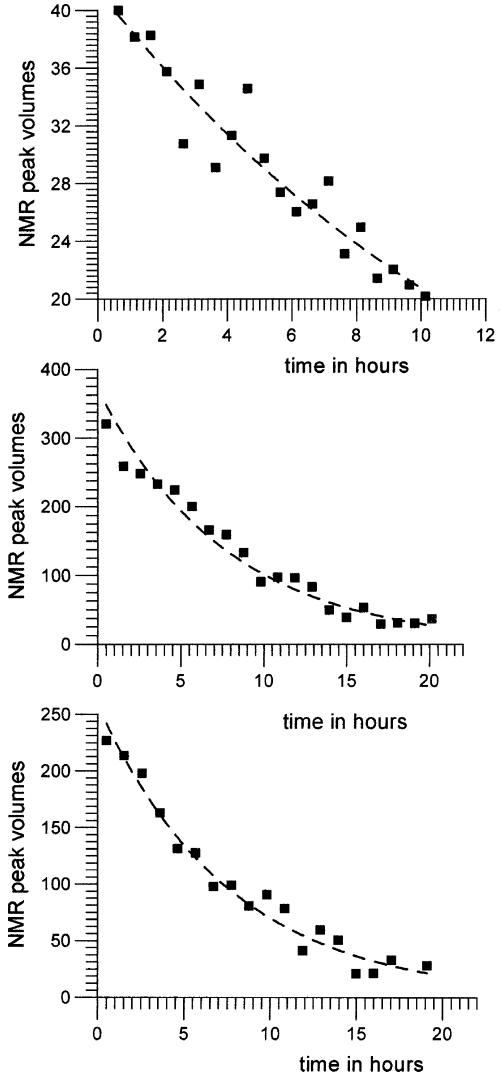

Figure 7. Integrated intensities (volumes) of NMR peaks as functions of time in the presence of 15 million Jurkat cells. Results of three experiments (~10 h, top; ~20 h, middle and bottom) are shown. Squares = intensities for peak at $^{1}H/^{15}N$, $\delta = 4.09/-68.0$, due to **1**; dashed lines = exponential fits. The peak at $^{1}H/^{15}N$, $\delta = 3.61/-80.5$, seen in the absence of cells, never appears.

9.3 ± 2.5 μM/h for the initial rate of decrease (standard error of fit given). Averaging the three, we obtain 7.6 ± 1.5 μM/h (average $\pm$ variance). Analysis of the data shown in Figure 7 (15 million Jurkat cells present) in the same way gave initial rates of decrease of 4.2 ± 0.8, 4.5 ± 1.6, and 5.8 ± 0.6 μM/h. Averaging the three, we obtain 4.8 ± 0.7 μM/h (average $\pm$ variance). This is significantly lower than the rate in the absence of cells. However, if the data for all t values are fitted to exponentials, the exponential parameter is essentially the same in the presence and absence of cells.

The interpretation of these results is that **1** aquates to produce **4** and also reacts with some components of the culture medium. The species **4** also reacts with some components of the culture medium, but because **4** is being produced from **1**, the apparent rate of decay of the intensities for **4** is much slower. The products of the reactions of **1** and **4** with the medium are not seen in the NMR, either because the product molecules are of very high molecular weight or because there are too many different products and the concentration of any one is too low to be detected in the experiment. In the presence of 15 million cells, the peak arising from **4** is not observed in the HSQC NMR. In other experiments, not shown here, we have observed this peak when fewer than 5 million cells are present. The peak's absence indicates that **4** is removed from solution by the cells more rapidly than **1**.

The identity of a new signal at 3.98/−62.0, which appears after 8−10 h in the presence of cells, is unknown. However, we note that measured cell viability remains high for ~12 h, but it decreases rapidly for 12−20 h, indicating that apoptosis is taking place at these times. This suggests that the signal at 3.98/−62.0 is associated with a species formed by the reaction of **1** with components released from the cells to the medium during apoptosis.

Discussion

In this work, we show that the amount of Pt bound to genomic DNA of Jurkat cells correlates linearly with the AUC, calculated as the product of the initial concentration of cisplatin in the medium and the exposure time to

the drug. The correlation is slightly less good if the AUC is calculated as $\int C\,dt$, where C is the actual [cisplatin]. The NMR experiments show that the drug (form **1**) slowly hydrolyzes to produce the mono-aquated form **2**, which at the pH of the medium, forms mainly the deprotonated complex, **4**. When 5 million or more cells are present in the medium, the NMR studies indicate that hydrolysis of **1** is occurring but **4** is not observed. That this signal is not observed in the presence of cells could be due to electrostatic or covalent binding of the mono-aquo complex to the surface of the cell and/or to the reaction of this compound with a high molecular weight molecule in the cytoplasm.

Other workers have observed that aquated forms of cisplatin are preferentially taken up by cells. Jennerwein and Andrews (*38*) and later Howell and co-workers (*39*) exposed human ovarian, head, and neck carcinoma cells to mixtures containing the aquated forms of cisplatin and measured the amount of Pt bound to DNA. They found that as compared to cisplatin itself, aquated forms of the drug are more effective at platinating DNA. In a later study, Pereira-Maia and Garnier-Suillerot (*40*) showed that the diaquated products, **5** and **6**, compounds not observed in our experiments, are taken up by small lung cancer cells at a rate ~40 times faster than cisplatin. Although **5** and **6** are not likely to form in media with high chloride concentrations, e.g., culture media or blood, the compound appears to be actively pumped into the cell by a transport mechanism. Recently, it has been shown that proteins responsible for the transport of copper into the cell may also be responsible for the active uptake of Pt (*5*, *41*). Clearly, determining the mechanism by which **2** (**4**) is removed from solution by Jurkat cells will require additional study.

Although the rate of decrease of [**1**] over time is about the same in the presence and absence of cells, the initial rate of decrease of [**1**] is larger when no cells are present. The reason for this may be that **1** reacts with some components of the culture medium, as well as aquating to **4**, and that some of the components of the meduim are absorbed by the cells at early times. The species **4** also reacts with components of the culture medium, but because **4** is being formed from **1** at the same time, the apparent rate of decrease of [**4**] is much smaller than that of [**1**].

The most important observation is that **4** never appears when 5 million or more cells are present. This shows that **4** is removed from solution by the cells much faster than **1**. The RPMI medium contains ~3 μM GSH and ~370 μM cysteine, both of which are good nucleophiles for Pt. The fact that these compounds do not react with Pt species to produce products having S trans to $^{15}NH_3$ (δ ^{15}N ~ −40 ppm) (*28*) is an indication that in the culture medium these thiols are in their less reactive disulfide forms.

Theoretical Model

Having determined that platination is proportional to AUC for Jurkat cells in culture and having found that cells remove **2** (**4**) more efficiently than **1** from the extracellular solution, we refined our kinetic model (*21*) of cisplatin binding to cellular DNA. The model considers the important processes involved in bringing extracellular Pt to nuclear DNA, where it forms the lesions, which

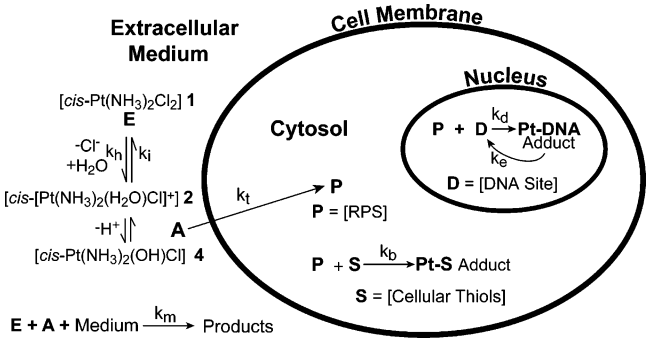

Figure 8. Model showing the important processes leading to the platination of genomic DNA by cisplatin. The definitions of the terms used in the model are as follows: E, extracellular concentration of cisplatin, **1**; k_h, rate constant for hydrolysis of **1** to the mono-aquo form, **2**; A, sum of concentrations of **2** and **4**; k_i, rate constant for the conversion of **2** to **4**; k_m, rate constant for the reaction of **1**, **2**, and **4** with components in the medium; k_t, rate of uptake of **2** and **4** into the cell; P, cytosolic concentration of RPS; D, number of available sites on DNA for RPS; k_d, rate constant for the reaction of RPS with DNA; S, total concentration of cellular thiols; k_b, rate constant for the reaction of cellular thiols with RPS; k_e = rate constant for repair.

lead to apoptosis. The processes considered in the model are shown in Figure 8 and discussed below. It is recognized that each process may involve several chemical or biochemical reactions.

(i) The first process is the aquation of the dichloro species, **1**, to **2**, which becomes a mixture of **2** and **4**. The rate of aquation is k_hE, where E is the concentration of **1** and $k_h = 0.205\ h^{-1}$, as measured in the present study and elsewhere (*29*). The reverse rate is $k_i[Cl^-][\mathbf{2}]$, where k_i can be calculated from k_h and the measured equilibrium constant (*29*). (ii) As has been shown in this work, the monoaquo compound **2** (**4**) is removed from the extracellular solution by Jurkat cells. Ghezzi et al. (*42*) have recently measured the amount of Pt taken up by human MCF-7 breast cancer cells exposed to cisplatin. They confirmed that the uptake rate is proportional to E, even at high concentrations and times. Although they did not determine the form of the Pt entering the cells, it is reasonable to assume that it is the same as that removed from the solution by the cells. We use the value of the rate constant that they determined, $k_t = 4.2 \times 10^{-13}$ mol $M^{-1}\ h^{-1}$ per cell. Measurements in our laboratory with Jurkat cells exposed to cisplatin gave a similar value for this rate constant (Centerwall and Tacka, personal communication). The rate constant for Pt entering the cell interior (as compared to becoming covalently bound to the outside) is certainly smaller than 4.2×10^{-13} mol $M^{-1}\ h^{-1}$ per cell, but we know of no way to determine it. This value of k_t is multiplied by the number of cells and divided by the reaction volume ($V_{reaction} = 20$ mL) to get the rate of decrease of extracellular Pt concentration or divided by a cell volume ($V_{cell} = 1$ pL) to obtain the rate of increase of intracellular concentration. (iii) In the cytosol, where $[Cl^-]$ is much lower than outside the cell, free **2** (**4**) may lose chloride to form **5** (**6**). For the model, we consider all species in the cytosol together as reactive platinum species (RPS), the concentration of which (P) is determined by k_t and the extracellular concentration of **2** (**4**). (iv) The RPS may react with thiols such as GSH or MT, which may prevent platination of nuclear DNA (*2*, *7*−*9*, *43*). The reaction is assumed second-order, with rate k_bSP where S is the concentration of thiol groups in

the cytosol, ~3 mM for GSH plus MT (*43*), and k_b is 0.013 M^{-1} s^{-1} for GSH and 0.65 M^{-1} s^{-1} for MT reacting with **1** (*21*, *44*, *45*). The rates of reaction of **1** and **4** with nucleophiles should be similar because the leaving groups are Cl^- and OH^-, respectively (*46*), so we approximate the rate constant for reaction of **4** with cellular thiols as 0.65 M^{-1} s^{-1}. (v) We assume that Pt crosses the nuclear membrane by passive diffusion (*21*, *47*) and then reacts with nuclear DNA by a second-order reaction. The rate of formation of Pt−DNA adducts is given by k_dPD, P being the intracellular RPS concentration and D being the number of available DNA sites to which the RPS can bind. The rate constant for the mono-aquo complex at pH 6.0 at 25 °C to form a monoadduct with guanine in an oligonucleotide duplex in vitro has been measured as 1.06 M^{-1} s^{-1} (*25*). However, this does not seem applicable to the cell because the rate measurements were made with both reactants uniformly distributed in solution, so that the process by which the RPS reaches the compartment containing the DNA (the nucleus) was not included. Rather than add another parameter to the model, we have chosen to consider transport of RPS to the interior of the nucleus and subsequent reaction with DNA sites as a single process, with rate $-dD/dt = k_dDP$. (vii) The initial concentration of exposed DNA sites, D_0, may be estimated as follows. The preferred binding site is GG (*1*) and about 1/5 of the 5×10^9 bases in the nuclear DNA are Gs, so there are about 2×10^8 GG binding sites. Estimating that only about 1% of the bases are exposed to attack by RPS and that there are other binding sites, we estimate D_0 as 3×10^6. Because the number of Pt adducts is always much less than D_0, D remains approximately equal to D_0, which means only the value of k_dD_0, and not the value of D_0, is important. Using the estimated value of D_0, we choose the value of k_d to give platination rates comparable to those measured in the AUC experiments described here. (viii) All species outside the cell react with the medium, with a first-order rate constant $k_m = 0.101$ h^{-1}. The value of k_m is obtained from NMR measurements of the total [cisplatin] ($E + A$) as a function of time in the absence of cells, where A is the sum of the concentrations of **2** and **4**; $E + A = c \exp(-k_mt)$. (ix) Finally, we write the rate of repair as $k_e(D_0 - D)$, since $D_0 - D$ is the number of adducts. Repair removes Pt from DNA, increasing D, but does not return the Pt to the pool of intranuclear RPS. The value of k_e can be estimated from measurements on neuroblastoma cells by Hagrman and Dubowy (personal communication). They found that when there were ~30 Pt−DNA adducts per 10^6 nts immediately after incubation with cisplatin, there were ~6 Pt−DNA adducts per 10^6 nt 4 h later. Thus, $6/30 = \exp(-4k_e)$ and $k_e = 0.4$ h^{-1}. For the present calculations, repair is numerically unimportant.

The differential equations resulting from these processes are now given. The concentration of **1**, E, changes because of reaction with the medium and conversion to the aquated forms (**2**, **4**), the total concentration of which is denoted by A:

$$\frac{dE}{dt} = -k_hE - k_mE + k_i[Cl^-]A\frac{[H^+]}{K_a + [H^+]} \qquad (1)$$

Here, K_a is the acid ionization constant of the chloro-aquo compound **2**. The factor $[H^+]/(K_a + [H^+])$ is required because form **1** interconverts with form **2** only (not form **4**). Also

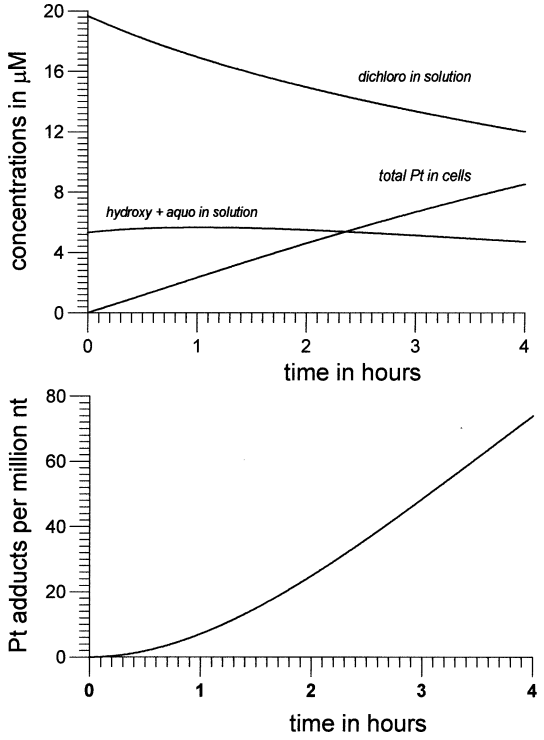

Figure 9. Results of calculations using the model of Figure 8. The initial concentration of cisplatin, **1**, = 65 μM. The rate of transport of aquated cisplatin into a cell is k_tA per cell where A is the concentration (M) of aquated cisplatin (**2** + **4**) outside the cells and $k_t = 4.2 \times 10^{-13}$ mol h^{-1} M^{-1}. Other rate constants are as follows: $k_h = 0.205$ h^{-1} (aquation), $k_i = 24.1$ M^{-1} h^{-1} (reverse to aquation), $k_m = 0.101$ h^{-1} (reaction with medium), $k_b = 0.65$ M^{-1} h^{-1} (reaction of Pt with thiols), $k_d = 50$ M^{-1} h^{-1} per site (reaction of Pt with DNA), and $k_e = 0.4$ h^{-1} (repair). The number of available sites is $D_0 = 3 \times 10^6$. Upper panel: curves show the concentrations of extracellular cisplatin, **1**, chloro-aquo species **2** + chloro-hydroxy species **4**, and intracellular Pt. Lower panel: calculated number of Pt−DNA adducts as a function of time. The slope (rate of formation of adducts) is constant for $t >$ ~0.5 h.

$$\frac{dA}{dt} = k_hE - k_mA - k_i[Cl^-]A\frac{[H^+]}{K_a + [H^+]} - k_tA\frac{N_{cells}}{V_{reaction}} \qquad (2)$$

$$\frac{dP}{dt} = k_tA\frac{1}{V_{cell}} - k_bPS - k_dPD \qquad (3)$$

$$\frac{dD}{dt} = -k_d'PD + k_e(D_0 - D) \qquad (4)$$

$$\frac{dS}{dt} = -k_bPS \qquad (5)$$

Note that dP/dt is in M/h, whereas dD/dt is in millions of sites/h. The ratio of k_d' to k_d is thus the cell volume ($V_{cell} = 10^{-12}$ L) multiplied by Avogadro's number and divided by 10^6, i.e., 6×10^5. Equations 1−5 are solved numerically using the Rkadapt function of MathCad, which uses the Runge−Kutta method with variable step size.

Figure 9 shows results obtained for an initial concentration of **1** of 25 μM, assuming 10 million cells present, as in the AUC measurements. The upper panel shows the concentrations of **1** and **2** + **4** outside the cell, as well

as the total concentration of Pt inside the cell, vs time. The concentration of Pt inside the cell becomes larger than that outside the cell. The concentration of **2** + **4** is always too small to be seen in the NMR measurements, even though these species are formed from **1**, because aquated cisplatin passes into the cell as rapidly as it is formed. At $t = 3$ h, corresponding to AUC = 75 μM h, the number of Pt−DNA adducts is 1.45×10^5, corresponding to 48.4 adducts per million nt (lower panel of Figure 9). This is calculated based on the total number of nts in the genome, not only those exposed to platination, to correspond with what is actually determined in the AUC experiments. The value of k_d, 7×10^3 h^{-1} M^{-1} per site, was chosen so that this agrees (see Table 1) with what is found experimentally.

The thiol concentration (not shown in Figure 9) decreases by less than 0.01%, even at 4 h. The extent of Pt−thiol reaction is small because the value of the rate constant k_b and the RPS concentration are small. The total number of Pt−DNA adducts is comparable to the number of Pt−thiol adducts and much less than the number of Pt atoms in the cytosol. In fact, only about 3% of the Pt in the cell has reacted with nuclear DNA at 3 h. This is about what is stated in the literature, that ~1% of the cellular Pt is bound to DNA (*42*). The total amount of Pt in the cell is mainly determined by the rate at which **2** or **4** enters the cell.

Calculations with our model show that with 5 million cells and an original total [cisplatin] of 65 μM, A never exceeds 15 μM. Because the sensitivity of the NMR experiment (see Figures 6 and 7) prevents measurement of concentrations below ~15 μM, this explains why the mono-aquo species is never detected in experiments with 15 million cells. Model calculations with $E_0 = 65$ μM show that with fewer than 5 million cells, A would exceed 15 μM and would be detectable. Experiments (not reported here) confirm this.

A series of calculations using this model with various values of E_0 and t show that the amount of platination is proportional to AUC except for very short times. As seen in Figure 9 (lower panel), the number of adducts grows at a constant rate for $t > 0.5$ h. For $t < 0.5$ h, concentrations of the chloro-aquo species inside and outside the cell vary rapidly and the rate is not constant. The constancy of the rate of adduct formation implies that the amount of platination is proportional to AUC.

Summary and Conclusions

In this report, we show that for Jurkat cells in culture exposed to cisplatin, the number of Pt adducts on DNA is proportional to AUC. Here, AUC is the area under the concentration vs time curve for unreacted (dichloro) cisplatin. The number of Pt−DNA adducts is measured immediately following exposure to drug. We also show that the number of DNA adducts correlates linearly with a decrease in respiration, measured 24 h after removal of drug; there is no effect on respiration immediately after drug exposure. The number of adducts also correlates linearly with the amount of DNA fragmentation, measured 24 h after drug exposure, and with cell viability.

We also report on the use of HSQC NMR to study the reactions of cisplatin, at concentrations approaching clinical relevance, in the presence and in the absence of cells. In the absence of cells (but with cell growth medium present), the dichloro form **1** is transformed into the mono-aquo species ($k_h = 0.205$ h^{-1} at 37 °C) because the chloride concentration, originally 154 mM in the cisplatin stock solution, is lowered to 104 mM in the culture medium. As seen in the HSQC NMR, the concentration of the mono-aquo species decreases because of this transformation and reaction with the components of the medium. In the presence of cells, the concentration of **1** also decreases (with a somewhat smaller initial rate than in the absence of cells), reflecting the transformation to the mono-aquo species. However, the signal for the latter is not seen because **2** (**4**) is removed from the medium by the cells as rapidly as it is formed, keeping its concentration too low to be measured in these experiments. From experiments of this type, it is possible to measure the rate at which the mono-aquo species is accumulated by cells.

We present a phenomenological model for platination of nuclear DNA by exposure to cisplatin. The processes included are aquation of cisplatin outside the cell, passage of the chloro-aquo species through the cell membrane, reaction of RPS in the cytosol with thiols, formation of adducts between RPS and accessible DNA sites in the nucleus, and DNA repair. We have measured values for the repair rate and for the rate constant for the hydrolysis of cisplatin at 37 °C in culture medium. From the equilibrium constant for hydrolysis (*29*), we derive the rate constant for the reverse reaction. The rate constant for the reaction of **4** with thiols at pH 7.4, k_b, was estimated to be the rate constant for the reaction of **1** with cellular thiols (*43*−*45*). The uptake rate for Pt, presumably in the form **2** or **4**, by human breast cancer cells has been measured (*42*) and is used as an estimate of the rate at which Pt enters Jurkat cells. The rate constant k_d for the reaction of Pt with nuclear DNA (actually the rate of Pt transport to the nuclear DNA followed by its reaction with DNA) is not known. It turns out that only k_dD is important, where D is the number of available Pt binding sites. Estimating D, we choose a value of k_d in the model to give a number of adducts comparable to what we found in the AUC experiments.

Despite the approximations and assumptions, the model helps us to understand our experimental results and indicates what processes are important. For example, the model shows under what circumstances the amount of platination of nuclear DNA is proportional to AUC. It also shows that most of the Pt in the cell remains unreacted. The fraction of intracellular Pt that reacts with intracellular thiols is quite small. This suggests that thiols contribute to cell protection (and cell resistance) in ways other than simply reacting with Pt before it reaches the nuclear DNA. However, it may be that too small a value was used for the rate constant k_b (our value was obtained from in vitro measurements). Rate constants for reaction of Pt drugs with some drug thiols are more than an order of magnitude larger (*44*, *48*).

In addition, the model explains why the chloro-aquo species is not seen in our NMR experiments with 5 million or more cells present and predicts correctly the maximum number of cells, which can be used if this species is to be seen. The NMR experiments show that the species preferentially removed from the culture medium by Jurkat cells is mostly the mono-aquated form of the drug, which, at neutral pH, is mostly deprotonated. Because forms of cisplatin with one or two bound water molecules are more reactive to nucleophiles than **1**, the

anticancer effects of cisplatin might be enhanced by administration of aquated forms of the drug directly to the tumor. The suggestion was made by Howell and coworkers (*39*) that a therapeutic strategy be based on regional intraarterial or intracavity administration of aquated cisplatin in combination with a systemic neutralizing agent.

It is known that the extracellular pH of tumors is in the range of 6.0−7.0, while the extra- and intracellular pH of normal tissue is ∼7.4 (*49*, *50*). Because complex **2** has a pK_a for deprotonation of 6.41, the relative amounts of **2** and **4** found in normal tissue and tumors must be different. Clearly, additional study will be necessary to determine if and to what extent pH effects associated with tumors might contribute to the remarkable effectiveness of cisplatin for treating cancer.

Acknowledgment. The technical assistance of Bonnie Toms with the cell culture and Corey Centerwall with some of the NMR experiments was greatly appreciated. We are also thankful to Dr. D. Kerwood for her help with the HSQC NMR measurements. The support of the Syracuse University Chemistry Department is also acknowledged.

References

(1) Cohen, S. M., and Lippard, S. J. (2001) Cisplatin: From DNA damage to cancer chemotherapy. *Prog. Nucleic Acid Res. Mol. Biol*. *67*, 93−130.

(2) Kartalou, M., and Essigmann, J. M. (2001) Mechanisms of resistance to cisplatin. *Mutat. Res*. *478*, 23−43.

(3) Crul, M., van Waardenburg, R. C., Beijnen, J. H., and Schellens, J. H. (2002) DNA-based drug interactions of cisplatin. *Cancer Treat. Rev*. *28*, 291−303.

(4) Samimi, G., Varki, N. M., Wilcznski, S., Safaei, R., Alberts, D. S., and Howell, S. B. (2003) Increase in expression of the copper transporter ATP7A during platinum drug-based treatment is associated with poor survival in ovarian cancer patients. *Clin. Cancer Res*. *9*, 5853−5859.

(5) Katano, K., Kondo, A., Safaei, R., Holzer, A., Samimi, G., Mishima, M., Kuo, Y.-M., Rochdi, M., and Howell, S. B. (2002) Acquisition of resistance to cisplatin is accompanied by changes in the cellular pharmacology of copper. *Cancer Res*. *62*, 6559−6565.

(6) Liu, J., Chen, H., Miller, D. S., Saavedra, J. E., Keefer, L. K., Johnson, D. R., Klaassen, C. D., and Waalkes, M. P. (2001) Overexpression of glutathione S-transferase II and multidrug resistance transport proteins is associated with acquired tolerance to inorganic arsenic. *Mol. Pharmacol*. *60*, 302−309.

(7) Boulikas, T., and Vougiouka, M. (2004) Recent clinical trials using cisplatin, carboplatin and their combination chemotherapy drugs (Review). *Oncol. Rep*. *11*, 559−595.

(8) Fuertesa, M. A., Castillab, J., Alonsoa, C., and Perez, J. M. (2003) Cisplatin biochemical mechanism of action: From cytotoxicity to induction of cell death through interconnections between apoptotic and necrotic pathways. *Curr. Med. Chem. 10*, 257−266.

(9) Siddik, Z. H. (2003) Cisplatin: Mode of cytotoxic action and molecular basis for resistance. *Oncogene 22*, 7265−7279.

(10) Ruden, C. M., Yang, Z., Shumaker, L. M., VanderWeele, D. J., Newkirk, K., Egorin, M. J., Zuhowski, E. G., and Cullen, K. J. (2003) Inhibition of glutathione synthesis reverses Bcl-2-mediated cisplatin resistance. *Cancer Res*. *63*, 312−318.

(11) Arnér, E. S. J., Nakamura, H., Sasada, T., Yodoi, J., Holmgren, A., and Spyrou, G. (2001) Analysis of the inhibition of mammalian thioredoxin, thioredoxin reductase, and glutaredoxin by cis-diamminedichloroplatinum (II) and its major metabolite, the glutathione-platinum complex. *Free Radical Biol. Med*. *31*, 1170−1178.

(12) Awasthi, S., Singhal, S. S., Sharma, R., Zimniak, P., and Awasthi, Y. C. (2003) Transport of glutathione conjugates and chemotherapeutic drugs by RLIP76 (RALBP1): A novel link between G-protein and tyrosine kinase signaling and drug resistance. *Int. J. Cancer 106*, 635−646.

(13) Ozawa, S., Suglyama, Y., Mitsuhashi, Y., Kobayashi, T., and Inada, M. (1988) Cell killing action of cell cycle phase-nonspecific antitumor agents is dependent on concentration−time product. *Cancer Chemother. Pharmacol*. *21*, 185−190.

(14) Ma, J., Verweij, J., Kolker, H. J., Van Ingen, H. E., Stoter, G., and Schellens, J. H. M. (1994) Pharmacokinetic-dynamic relationship of cisplatin in vitro: Simulation of a i.v. bolus and 3 and 20 h infusion. *Br. J. Cancer 69*, 858−862.

(15) Kurihara, N., Kubota, T., Hoshiya, Y., Otani, Y., Kumai, K., and Kitajima, M. (1995) Antitumor activity of cis-diamminedichloroplatinum (II) depends on its time x concentration product against human gastric cancer cell lines in vitro. *J. Surg. Oncol*. *60*, 238−241.

(16) Inaba, M., Tashiro, T., Sato, S., Ohnishi, Y., Tanisaka, K., Kobayashi, H., and Koezuka, M. (1996) In vitro-in vivo correlation in anticancer drug sensitivity test using AUC-based concentrations and collagen gel droplet-embedded culture. *Oncology 53*, 250−257.

(17) Levasseur, L. M., Slocum, H. K., Rustum, Y. M., and Greco, W. R. (1998) Modeling of the time-dependency of in vitro drug cytotoxicity and resistance. *Cancer Res*. *58*, 5749−5761.

(18) El-Kareh, A. W., and Secomb, T. W. (2003) A mathematical model for cisplatin cellular pharmacodynamics. *Neoplasia 5*, 161−169.

(19) Troger, V., Fischel, J. L., Formento, P., Gioanni, J., and Milano, G. (1992) Effects of prolonged exposure to cisplatin on cytotoxicity and intracellular drug concentration. *Eur. J. Cancer 28*, 82−86.

(20) Miyagi, Y., Kawanishi, K., Miyagi, Y., Yamada, S., Yamamoto, J., Kodama, J., Hongo, A., Yoshinouchi, M., and Kudo, T. (2001) Cytocidal effect and DNA damage of nedaplatin: A mathematical model and analysis of experimental data. *Cancer Chemother. Pharmacol*. *47*, 229−235.

(21) Sadowitz, P. D., Hubbard, B. A., Dabrowiak, J. C., Goodisman, J., Tacka, K., Aktas, M. K., Cunningham, M. J., Dubowy, R. L., and Souid, A.-K. (2002) Kinetics of cisplatin binding to cellular DNA and modulations by thiol-blocking agents and thiol drugs. *Drug Metab. Dispos*. *30*, 183−190.

(22) Tacka, K. A., Dabrowiak, J. C., Goodisman, J., Penefsky, H. S., and Souida, A.-K. (2004) Effects of cisplatin on mitochondrial function in Jurkat cells. *Chem. Res. Toxicol. 17*, 1102−1111.

(23) Davies, M. S., Berners-Price, S. J., and Hambley, T. W. (2000) Rates of platination of -AG- and -GA- containing double-stranded oligonucleotides: Effect of chloride concentration. *J. Inorg. Biochem*. *79*, 167−172.

(24) Davis, M. S., Berners-Price, S. J., and Hambley, T. W. (2000) Slowing of cisplatin aquation in the presence of DNA but not in the presence of phosphate: Improved understanding of sequence selectivity and the roles of monoaquated and diaquated species in the binding of cisplatin to DNA. *Inorg. Chem*. *39*, 5603−5613.

(25) Davis, M. S., Berners-Price, S. J., and Hambley, T. W. (1998) Rates of AG and GA containing double-stranded oligonucleotides: Insights into why cisplatin binds to GG and AG but not GA sequences in DNA. *J. Am. Chem. Soc*. *120*, 11380−11390.

(26) Marchán, V., Moreno, V., Pedroso, E., and Grandas, A. (2001) Toward a better understanding of the cisplatin mode of action. *Chem. Eur. J*. *7*, 808−815.

(27) Oehlsen, M. E., Qu, Y., and Farrell, N. (2003) Reaction of polynuclear platinum antitumor compounds with reduced glutathione studied by multinuclear (^{1}H, ^{1}H-^{15}N gradient heteronuclear single-quantum coherence, and ^{195}Pt) NMR spectroscopy. *Inorg. Chem*. *42*, 5498−5506.

(28) Barnham, K. J., Berners-Price, S. J., Guo, Z., Murdoch, P., and Sadler, P. J. (1996) NMR spectroscopy of platinum drugs: From DNA to body fluids. In *Platinum and Other Coordination Compounds in Cancer Chemotherapy 2* (Pinedo, H. M., and Schornagel, J. H., Eds.) pp 1−16, Plenum Press, New York.

(29) Berners-Price, S. J., and Appleton, T. (2000) The chemistry of cisplatin in aqueous solution. In *Platinum-Based Drugs in Cancer Chemotherapy* (Kelland, L. R., and Farrell, N., Eds.) pp 3−35, Humana Press Inc., Totowa, NJ.

(30) Davies, M. S., Thomas, D. S., Hegmans, A., Berners-Price, S. J., and Farrell, N. (2002) Kinetic and equilibria studies of the aquation of the trinuclear platinum phase II anticancer agent, [{*trans*-PtCl(NH$_3$)$_2$}$_2${*μ-trans*-Pt(NH$_3$)$_2$(NH$_2$(CH$_2$)$_6$NH$_2$)$_2$}]$^{+4}$ (BBR3464). *Inorg. Chem*. *41*, 1101−1109.

(31) Berners-Price, S. J., Frenkiel, T. A., Frey, U., Ranford, D. J., and Sadler, P. J. (1992) Hydrolysis products of cisplatin: pK_a determinations via [^{1}H-^{15}N] NMR spectroscopy. *J. Chem. Soc. Chem. Commun*. 789−791.

(32) Kukushkin, V. Y., Oskarsson, A., Elding, L. I., and Farrell, N. (1998) Facile synthesis of isomerically pure cis-dichlorodiammineplatinum (II), cisplatin. *Inorg. Synth*. *32*, 141−144.

(33) Allison, D. C., and Ridolpho, P. (1980) Use of trypan blue assay to measure the deoxyribonucleic acid content and radioactive labeling of viable cells. *J. Histochem. Cytochem*. *28*, 700−703.

(34) Souid, A.-K., Tacka, K. A., Galvan, K. A., and Penefsky, H. S. (2003) Immediate effects of anticancer drugs on mitochondrial oxygen consumption. *Biochem. Pharmacol*. *66*, 977−987.

(35) Lo, L.-W., Koch, C. J., and Wilson, D. F. (1996) Calibration of oxygen dependent quenching of the phosphorescence of Pd-*meso*-tetra (4-carboxyphenyl) porphine: A phosphor with general application for measuring oxygen concentration in biological systems. *Anal. Biochem*. *236*, 153−160.

(36) Gong, J., Traganos, F., and Darzynkiewicz, Z. (1994) A selective procedure for DNA extraction from apoptotic cells applicable for gel electrophoresis and flow cytometry. *Anal. Biochem*. *218*, 314−319.

(37) Mimnaugh, E. G., Yunbam, M. K., Li, Q., Bonvini, P., Hwang, S.-G., Trepel, J., Reed, E., and Neckers, L. (2000) Prevention of cisplatin-DNA adduct repair and potentiation of cisplatin-induced apoptosis in ovarian cancer cells by proteasome inhibitors. *Biochem. Pharmacol. 60*, 1343−1354.

(38) Jennerwein, M., and Andrews, P. A. (1994) Drug accumulation and DNA platination in cells exposed to aquated cisplatin species. *Cancer Lett*. *81*, 215−220.

(39) Zheng, H., Fink, D., and Howell, S. B. (1997) Pharmacological basis for a novel therapeutic strategy based on the use of aquated cisplatin. *Clin. Cancer Res*. *3*, 1157−1165.

(40) Pereira-Maia, E., and Garnier-Suillerot, A. (2003) Impaired hydrolysis of cisplatin derivatives to aquated species prevents energy-dependent uptake in GLC4 cells resistant to cisplatin. *J. Biol. Inorg. Chem*. *8*, 626−634.

(41) Ishida, S., Lee, J., Thiele, D. J., and Herskowitz, I. (2002) Uptake of the anticancer drug cisplatin mediated by the copper transporter Ctr1 in yeast and mammals. *Proc. Natl. Acad. Sci. U.S.A. 99*, 13963−13965.

(42) Ghezzi, A. R., Aceto, M., Cassino, C., Gabano, E., and Osella, D. (2004) Uptake of antitumor platinum(II) complexes by cancer cells, assayed by inductively coupled plasma mass spectrometry (CIP-MS). *Inorg. Biochem. 98*, 73−78.

(43) Eastman, A. (1991) Mechanisms of resistance to cisplatin. *Cancer Treat. Res*. *57*, 233−249.

(44) Dabrowiak, J. C., Goodisman, J., and Souid, A.-K. (2002) Kinetic study of the reaction of cisplatin with thiols. *Drug Metab. Dispos. 30*, 1378−1384.

(45) Hagrman, D. E., Goodisman, J., Dabrowiak, J. C., and Souid A. K. (2003) Kinetic study on the reaction of cisplatin with metallothionein. *Drug Metab. Dispos. 31*, 916−923.

(46) Basolo, F., and Pearson, R. G. (1967) *Mechanisms of Inorganic Reactions*, 2nd ed., Wiley, New York.

(47) Falerio, L., and Lazebnik, Y. (2000) Caspases disrupt the nuclear-cytoplasmic barrier. *J. Cell. Biol*. *151*, 951−959.

(48) Treskes, M., Holwerda, U., Klein, I., Pinedo, H. M., and Van der Vijgh, W. F. The chemical reactivity of the modulating agent WR2721 (ethiofos) and its main metabolites with the antitumor agents cisplatin and carboplatin. *Biochem. Pharmacol. 47*, 2125−2130.

(49) Kozin, S. V., Shkarin, P., and Gerweck, L. E. (2001) The cell transmembrane pH gradient in tumors enhances cytotoxicity of specific weak acid chemotherapeutics. *Cancer Res*. *61*, 4740−4743.

(50) Stubbs, M., McSheehy, P. M., Griffiths, J. R., and Bashford, C. L. (2000) Causes and consequences of tumor acidity and implications for treatment. *Mol. Med. Today 6*, 15−19.

TX0498760